

Saline-Enhanced Radiofrequency Thermal Ablation of the Lung: A Feasibility Study in Rabbits

Jeong Min Lee, MD^{1,2}
Sang Won Kim, MD¹
Chun Ai Li, MD¹
Ji Hyun Youk, MD¹
Young Kon Kim, MD¹
Zhe Wu Jin, MD³
Myoung Ja Chung, MD⁴
Mi Suk Lee, MD⁵

Index terms :

Lung CT, interventional procedures
Radiofrequency, tissue ablation
Animal experiment

Korean J Radiol 2002 ; 3:245-253

Received April 8, 2002; accepted after revision September 9, 2002.

¹Department of Radiology, Chonbuk National University Medical School;

²Department of Radiology, Seoul National University Hospital; Departments of ³General Surgery and ⁴Surgical Pathology, Chonbuk National University Medical School; ⁵Department of Radiology, Yangji Hospital

Address reprint requests to:

Jeong-Min Lee, MD, Department of Diagnostic Radiology, Seoul National University Hospital, 28 Yongon-dong, Chongno-gu, Seoul 110-744, Korea.
Telephone: (822) 760-2510
Fax: (822) 743-6385
e-mail: jmlshy@naver.com

Objective: To assess the feasibility and safety of CT-guided percutaneous transthoracic radiofrequency ablation (RFA) with saline infusion of pulmonary tissue in rabbits.

Materials and Methods: Twenty-eight New Zealand White rabbits were divided into two groups: an RFA group (n=10) and a saline-enhanced RFA (SRFA) group (n=18). In the RFA group, percutaneous RFA of the lung was performed under CT guidance and using a 17-gauge internally cooled electrode. In the SRFA group, 1.5 ml of 0.9% saline was infused slowly through a 21-gauge, polytetrafluoroethylene-coated Chiba needle prior to and during RFA. Lesion size and the healing process were studied in rabbits sacrificed at times from the day following treatment to three weeks after, and any complications were noted.

Results: In the SRFA group, the mean diameter (12.5 ± 1.6 mm) of acute RF lesions was greater than that of RFA lesions (8.5 ± 1.4 mm) ($p < .05$). The complications arising in 12 cases were pneumothorax (n=8), thermal injury to the chest wall (n=2), hemothorax (n=1), and lung abscess (n=1). Although procedure-related complications tended to occur more frequently in the SRFA group (55.6%) than in the RFA group (20%), the difference was not statistically significant ($p = .11$).

Conclusion: Saline-enhanced RFA of pulmonary tissue in rabbits produces more extensive coagulation necrosis than conventional RFA procedures, without adding substantial risk of serious complications.

Image-guided radiofrequency thermal ablation is a rapidly evolving, minimally invasive technique used for the treatment of focal malignant diseases (1–4). In this respect, promising results have been reported in cases involving various solid tumors in different organs, especially in the treatment of primary and secondary hepatic malignancies (5–12). The recently published results of radiofrequency ablation (RFA) for the treatment of primary and secondary lung malignancies are encouraging, though the two reported studies included only a few cases and follow-up was limited (13, 14). The potential benefits of these techniques compared with conventional surgical options or radiation therapy for the treatment of lung malignancies include tumor ablation in nonsurgical candidates, reduction of the morbidity associated with surgery or radiation therapy, and the fact that the procedure can be performed on an outpatient basis.

The considerable differences in tissue characteristics between the lung and other solid organs such as the liver or kidneys influence the outcome of RFA, and this must be borne in mind when the technique is used for the treatment of lung malignancies. First, air-containing lung tissue has a naturally high tissue impedance, and the creation of a

surgical margin around the tumor may thus be difficult, a fact which might be related to the high local recurrence rate (6, 15–17). In addition, in cases of oval-shaped lung tumor, in which additional placement of an RF electrode at the tumor margin may be needed if complete necrosis is to be achieved, projection of the electrode tip into lung tissue could induce a rapid increase in impedance and limit the effectiveness of RFA. Furthermore, to prevent pneumothorax, the number of electrical passes through the pleural surface should be minimized during RF ablation of the lung. To minimize possible local recurrence at the tumor margin, and thus the occurrence of pneumothorax, it is, therefore, necessary to induce more extensive thermal necrosis with one RF ablation procedure. Previous studies of saline-enhanced RFA of the liver (18, 19) have shown that the use of saline allows thermal energy to spread further and faster in tissue, and increases tissue ionicity, thereby permitting greater current flow. To our knowledge, however, the literature contains the report of saline-enhanced RFA of the lung.

The purpose of this investigation is to assess the technical feasibility and safety of CT-guided transthoracic RFA with simultaneous saline infusion in rabbit lung.

MATERIALS AND METHODS

Animal Preparation

Twenty-eight male New Zealand white rabbits weighing 2.5–3 kg were anesthetized by intramuscular injection of 50 mg/kg ketamine hydrochloride (Ketamine[®]; Yuhan, Seoul, Korea) and 5 mg/kg xylazine (Rumpun[®]; Bayer Korea, Ansan, Korea) prior to RFA and other procedures. Booster injections of up to one-half of the initial dose were administered as needed. The upper back and lower abdominal areas were shaved and sterilized, and each animal was placed in the prone position on the CT table.

To assess the feasibility and safety of saline-enhanced RFA of normal lung parenchyma compared to conventional RFA, rabbits were allocated to either the RFA group (n=10) or the saline-enhanced RFA (SRFA) group (n=18). In addition, to compare the histopathologic change in lung parenchyma following SRFA and the occurrence of delayed complications, the rabbits in the SRFA group were allocated to either an acute (n=10) or subacute subgroup (n=8), and sacrificed at different time intervals after the procedure. In the RFA group (n=10) and the acute subgroup of the SRFA group (n=10), unilateral lung RFA was performed in 20 rabbits and all were sacrificed on the day of the procedure. During the subacute phase, eight rabbits were sacrificed on day 7 (n=2), or day 10 (n=2), and at two (n=2) or three weeks (n=2) after RFA.

RF Ablation Procedure

A Somatom Plus-4 CT scanner (Siemens, Erlangen, Germany) was used to obtain axial scans (2-mm slice thickness and 1.0–1.5 pitch) of the entire lung field, and the target portion and appropriate approach route for saline infusion and RFA were thus determined. In the saline infusion group, a polyteflon-coated 21-gauge Chiba needle (M.I.Tech, Seoul, Korea) was used for 0.9% saline infusion before and during the application of RF energy.

An internally cooled, 17-gauge electrode (Radionics; Burlington, Mass., U.S.A.) with a 1- or 2-cm active tip was placed in the target area of the lung under CT guidance, and the Chiba needle was inserted using the tandem technique (20). To maximize the effects of saline instillation, the tip of the needle was placed 3 mm posterior to the tip of the RF electrode. To confirm the position of the needle and the electrode in the target area, CT scanning was performed. Saline (0.5 mL) was then infused at a rate of 0.1 mL/sec prior to the application of RF energy, and to avoid bronchial aspiration, 1 mL saline at a rate of 0.05 mL/sec was also infused during RFA after frequent pulsing began. An electrode with a 1-cm active tip was used in rabbits in the RFA and SRFA groups to evaluate the immediate effects of RFA, while the electrode used in the subacute subgroup to evaluate histopathologic change and delayed complications had a 2-cm active tip.

Lesions were created using a 500-kHz RF generator (CC-3; Radionics) capable of producing 200 W of power. For analyzing the adverse effects of RF energy on lung parenchyma, ablated lesions were induced in the central portion of the lung in 14 rabbits and in its peripheral portion in the other 14. During the procedure, a thermocouple embedded within the electrode tip continuously measured the local tissue temperature, and tissue impedance was monitored by circuitry incorporated within the generator. A peristaltic pump (Watson-Marlow; Medford, Mass., U.S.A.) was used to infuse normal saline solution at 0 °C into the lumen of the electrode at a rate of 10–25 mL/min, and this was sufficient to maintain a tip temperature of 20–25 °C. When the desired current could not be applied due to a rapid elevation of impedance suggestive of tissue boiling, the generator automatically switched to the pulsed-RF technique (21). Power output was set at 30 W, and RF energy was applied for approximately five minutes on the basis of our earlier study findings (22).

Postprocedural Follow-up

Using the same scanner and starting two hours after RFA (day 0), Spiral CT scans were obtained to monitor the effects of ablation and to observe morphological change in the lesions at weeks 1, 2, and 3 after RFA. Axial scans (2-

mm slice thickness and 1.0–1.5 pitch) of both the lung and upper abdomen, including the kidneys, were obtained before and after the injection of contrast medium (6–9 mL, Ultravist 370[®]; Schering, Berlin, Germany) at a rate of 1 mL/sec through the ear vein. Post-contrast CT scans were obtained 30 and 60 secs after contrast administration. The diameters of the ablated lesions were measured on PACS images by one radiologist using an electric caliper.

Imaging Analysis: Two radiologists experienced in body imaging reviewed pre- and post-ablation CT images of all animals. They interpreted these side by side, and in each case reached a consensus. Each RFA lesion was evaluated in terms of its location, size and shape, attenuation change, and the presence of hemorrhage or air in the pleural cavity, and then classified as either central (inner 2/3) or peripheral (outer 1/3), depending on its location. To ensure that the changes noted were not present before RFA, the post- and preprocedural CT findings were compared.

Histopathologic examination: After spiral CT examination, rabbits were sacrificed at various points in time by injection of an overdose of Ketamine and Xylazine, and their lungs were harvested. The gross specimens obtained were dissected in planes similar to those of the spiral CT scans, and were examined. For macroscopic examination, two observers, who reached a consensus, used calipers to measure the central discolored region of coagulation necrosis in each pathologic specimen. Tissues were then fixed in 10% formalin for routine histologic examination, and final processing for light microscopic study involved paraffin sectioning and hematoxylin-eosin (HE) staining. Tissues obtained from all treatment areas were analyzed for nonviability, their histologic appearance, and demarcation from surrounding viable tissue. A surgical pathologist and a radiologist evaluated the gross and microscopic findings at each RFA site, and reached a consensus.

Data Analysis

The technical aspects of RFA (namely, total time needed for the procedure and current or impedance changes occurring) and complications arising were compared for both techniques. For all statistical analysis, SPSS 9.0 computer software (SPSS Inc., Chicago, Ill., U.S.A.) was used. The size of the acute RF lesions in the two groups was compared using an unpaired Student's *t* test. All contingency data were analyzed using the chi-square test, or Fisher's exact test for fewer than five observed events. For all statistical analysis, a *p* value of less than 0.05 was considered statistically significant.

RESULTS

RFA was technically successful in all instances, and 28 lesions were created with or without saline infusion. No anesthesia- or procedure- related deaths occurred.

Technical Parameters

Since the tip of the RF electrode or Chiba needle was easily localized at CT, its positioning was not difficult. The time required for correct needle placement ranged from 1.5 to 3.5 (mean, 2.3 ± 0.6) minutes for RFA and from 2.7 to 4.5 (mean, 3.4 ± 1.5) minutes for SRFA (*p* = .04).

In the RFA group, mean initial tissue impedance was $187 \pm 24 \Omega$, and in the SRFA group, after instillation of 0.5 mL of normal saline, the reading decreased to $134 \pm 24 \Omega$ (*p* < .05). In the RFA group, tissue impedance changed markedly (from 200 to 1000 Ω) during the procedure and frequently induced activation of the pulsing technique, whereas in the SRFA group, impedance showed no notable change (range, 100–500 Ω). Without saline infusion, as in the RFA group, impedance rose abruptly within a mean period of 20 ± 4.5 seconds. This automatically initiated RF pulsing, which was followed by alternating 5–10-second periods of high-energy deposition and approximately 15-second periods of low energy deposition. With saline infusion prior to and during RFA (SRFA group), impedance remained constantly low (at approximately 100 Ω) during the first 1–2 minutes of RF energy instillation, but an abrupt rise which induced RF pulsing occurred during the second half of the procedure (at mean 107 ± 54 seconds). Additional infusion of saline after the initiation of RF pulsing led to a lower rise in impedance and extended the time of continuous RF energy application. Differences between the two groups in the duration of RF energy instillation before pulsing were statistically significant: 20 ± 4.5 vs. 107 ± 54 seconds (*p* < .05).

The Effects of Tissue Ablation, and Complications

In the SRFA and RFA groups, the mean maximum diameters of acute lesions induced by a 1-cm active tip, as measured in gross specimens, were 12.5 ± 1.6 and 8.5 ± 1.4 mm, respectively; this difference between the two groups was statistically significant (*p* < .05) (Table 1). In the SRFA group, the mean maximum diameter of subacute lesions induced by a 2-cm active tip was 21.3 ± 5.8 cm (*p* < .05).

The complications occurring after RFA are summarized in Table 2, and were as follows: pneumothorax (n=8); thermal injury to the chest wall (n=2); hemothorax (n=1); and lung abscess (n=1). Three pneumothoraces were large (with lung volume decrease due to pleural air collection

and clinically visible respiratory distress) and five were small (perilesional small air collection, with no evidence of respiratory distress). Complications tended to occur more frequently in the SRFA group (55.6%, 10/18) than in the RFA group (20%, 2/10), though the difference was not statistically significant ($p = .11$). However, complication rates varied between the two groups, depending on the location of the lesions. Among central lesions, large pneumothorax occurred in two rabbits in the RFA group (20%, 2/10) and in one in the SRFA group (5.6%, 1/18) ($p = .28$). Among peripheral lesions, on the other hand, the complication rate was much higher in the SRFA group (77.8%) than in the RFA group ($p = .02$). The complications involved included thermal injury to the chest wall, and one lung abscess.

The incidence rates of complications, namely 35.7%

(5/14) for centrally located lesions and 50% (7/14) for peripherally located lesions, did not differ significantly ($p =$

Table 1. Summary of Maximum Lesion Diameter Induced by Radiofrequency Ablation

Group	Diameter (mean \pm SD, mm)	p value
RFA group (n=10)	8.5 \pm 1.4	$p < .05^*$
SRFA group (n=18)		
Acute subgroup (n=10)	12.5 \pm 1.6	
Subacute subgroup (n=8)	21.3 \pm 5.8	$p < .05^+$

Note.— RFA=radiofrequency ablation, SRFA=saline-enhanced radiofrequency ablation, *difference between mean diameter of lesions in the RFA group and those in the acute subgroup of the SRFA group, [†]difference between mean diameter of lesions in the acute and subacute subgroups

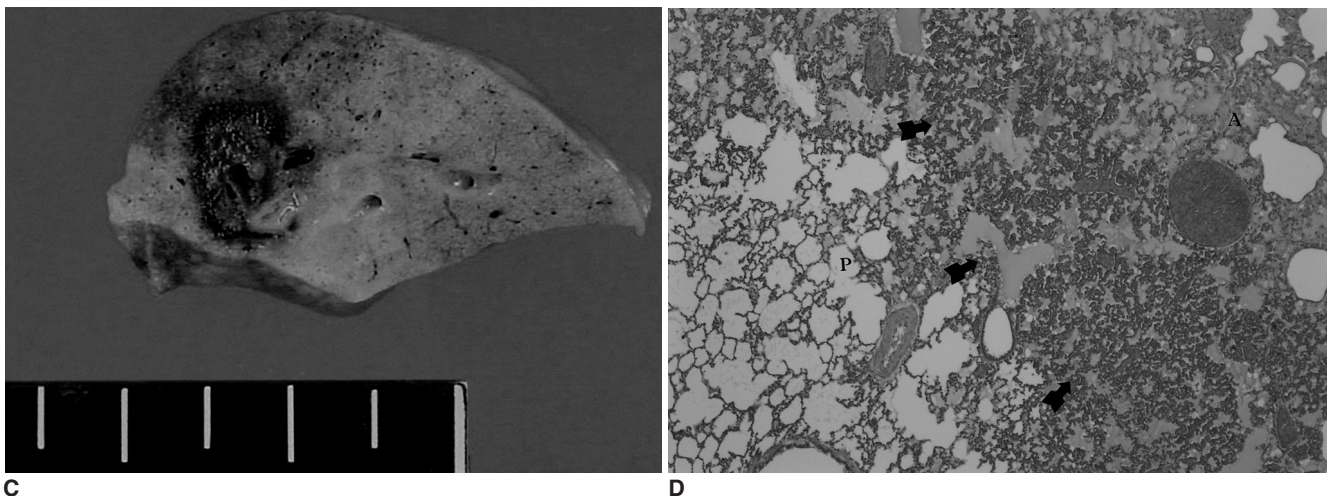
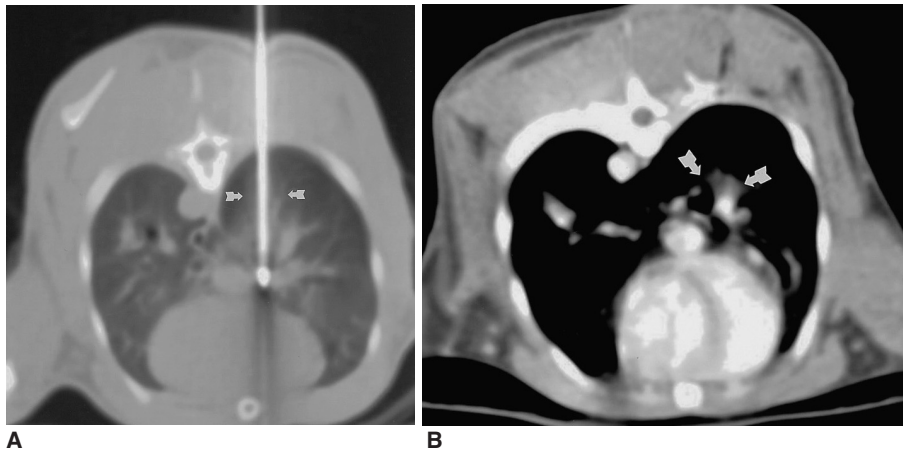


Fig. 1. Radiofrequency ablation in a rabbit in the radiofrequency group.
A. Computed tomographic section obtained during radiofrequency ablation. The right lower lobe is penetrated posteriorly by an electrode along which an ovoid opacity extends (arrows).
B. Contrast-enhanced CT scan obtained after the procedure depicts nonenhancing opacity (arrows) in the central portion of the right lobe. Note good enhancement of the pulmonary vessels in the area of ablation.
C. Gross specimen demonstrates an 8-mm central zone of coagulation necrosis surrounded by a dark-brown, 1-mm-thick hemorrhagic rim.
D. Microscopic image of the central ablation zone (A) shows that this contains pyknotic nuclei and eosinophilic cytoplasm, and that hemorrhagic congestion (arrows) has occurred at the border between the ablation area and normal pulmonary parenchyma (P).

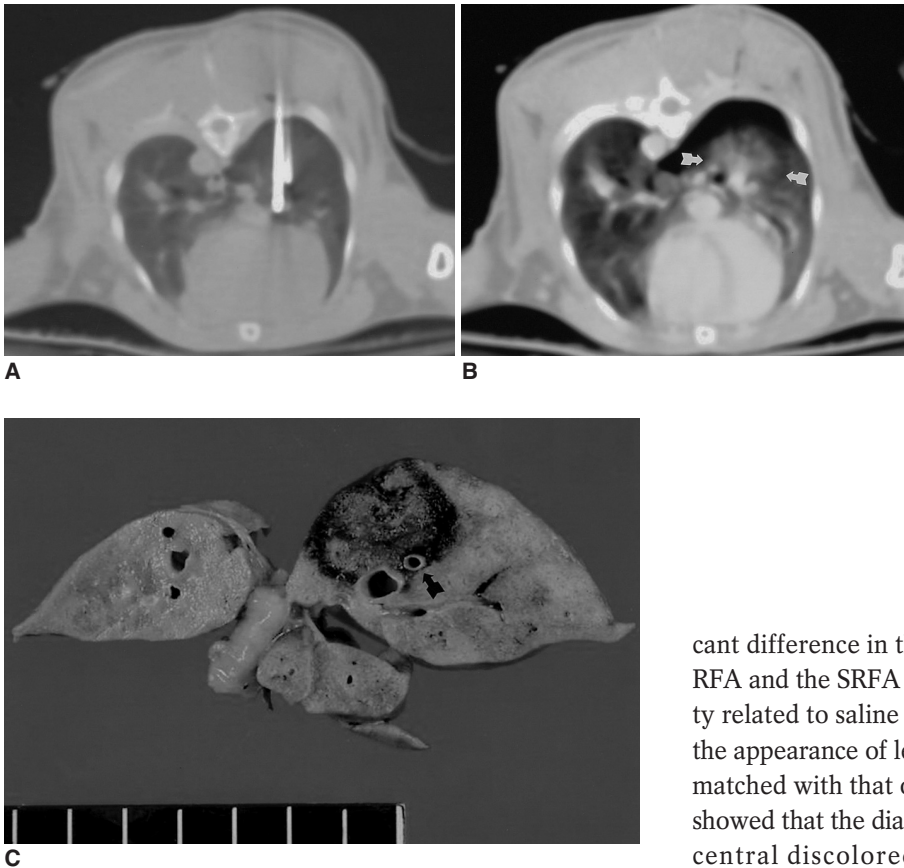


Fig. 2. Saline-enhanced radiofrequency thermal ablation in a rabbit in the saline-enhanced radiofrequency group.

A. A 17-gauge RF electrode and a 21-gauge coated Chiba needle have been placed in the right lower lobe of the lung. To maximize the effect of saline infusion, the tip of the needle is positioned 3mm posterior to the tip of the electrode.

B. Axial CT scan obtained after RF application shows a rounded opacity 12 mm in diameter (arrows), corresponding to coagulated alveoli and pneumothorax.

C. Gross specimen demonstrates a dark-brown area of coagulative necrosis surrounded by a peripheral hemorrhagic rim. Note the somewhat lobulated margin of the ablation zone, with focal sparing of the pulmonary artery (arrow).

.72), though the type of complication involved depended on the location of the ablated lesion. Although the incidence rate of pneumothorax (28.6%, 4/14) was not different between centrally and peripherally located lesions, large pneumothoraces (n=3) or hemothorax (n=1) occurred only in four central lesions (28.6%) adjacent to hilar vessels or bronchi. Major hemorrhage due to electrode penetration of vessels did not occur even where the lesion was located directly on a vessel.

Imaging and Histopathologic Findings

After RFA, unenhanced CT scanning revealed circumscribed hyperattenuated regions extending 5–8 mm from the portion of the inserted electrode (Fig. 1), while contrast-enhanced CT showed no enhancement in the region of altered pulmonary attenuation. Greater conspicuity of coagulated tissues was observed at wide window settings (level=500 HU, width = 2000 HU).

At CT imaging, thermal lesions appeared as hazy opacity in the soft tissue window (level=50 HU, width=350 HU) and ranged in diameter from 8 to 19 (mean, 12.6 ±4.3) mm (Figs. 1, 2). At CT imaging at a soft-tissue window setting, acute lesions were round or oval-shaped except in regions abutting pulmonary vessels, and there was no signifi-

cant difference in the shape of acute lesions between the RFA and the SRFA group. However, because of the opacity related to saline infusion in rabbits in the SRFA group, the appearance of lesions in the lung window was not well matched with that of gross specimens. Gross examination showed that the diameter of an acute lesion, measured as a central discolored region, was 7–14 (mean, 10.9 ± 1.8)mm, and the thickness of the peripheral rim was 1–2 mm. The mean difference in lesion size, as determined by CT scanning and pathologic examination, was 3 mm, which was not statistically significant (*p* > .05).

Histological examination of an acute lesion revealed a central charred zone with complete destruction of the parenchyma, including a small central cavity where tissue had been lost. Surrounding this were two zones of eosinophilic coagulative necrosis and a peripheral hemorrhagic rim (Figs. 1, 2). There was sharp cut-off between ablated lesions and normal lung. Outside this area, viable lung containing acute inflammatory cell infiltrate was present.

One to two weeks following RFA, surrounding tissue was becoming organized into granulation tissue, with an increase of fibroblasts and macrophages and dilatation of blood vessels at the perimeter of the lesion (Fig. 3). In a lesion’s central zone, typical findings of coagulation necrosis were observed. In centrally located lesions, fibrotic change was identified in the peribronchial area. At three weeks, granulation tissue had achieved progressive ingrowth into the original area of necrosis, and was replacing it, and there was sharp cut-off between the lesion and normal tissue. The final appearance was of a nodule comprised of central coagulation necrosis surrounded by a fibrous capsule.

DISCUSSION

Lung cancer is among the most commonly occurring malignancies in the world and is one of the few that continues to show an increasing incidence (23, 24). Although surgical

resection is acknowledged to be the treatment of choice and the only therapy with any prospect of cure or long-term survival, in practice a considerable percentage of patients with lung cancer are not eligible for surgical intervention due to the advanced stage of the disease, their limited pulmonary functional reserve, co-morbidities or ad-

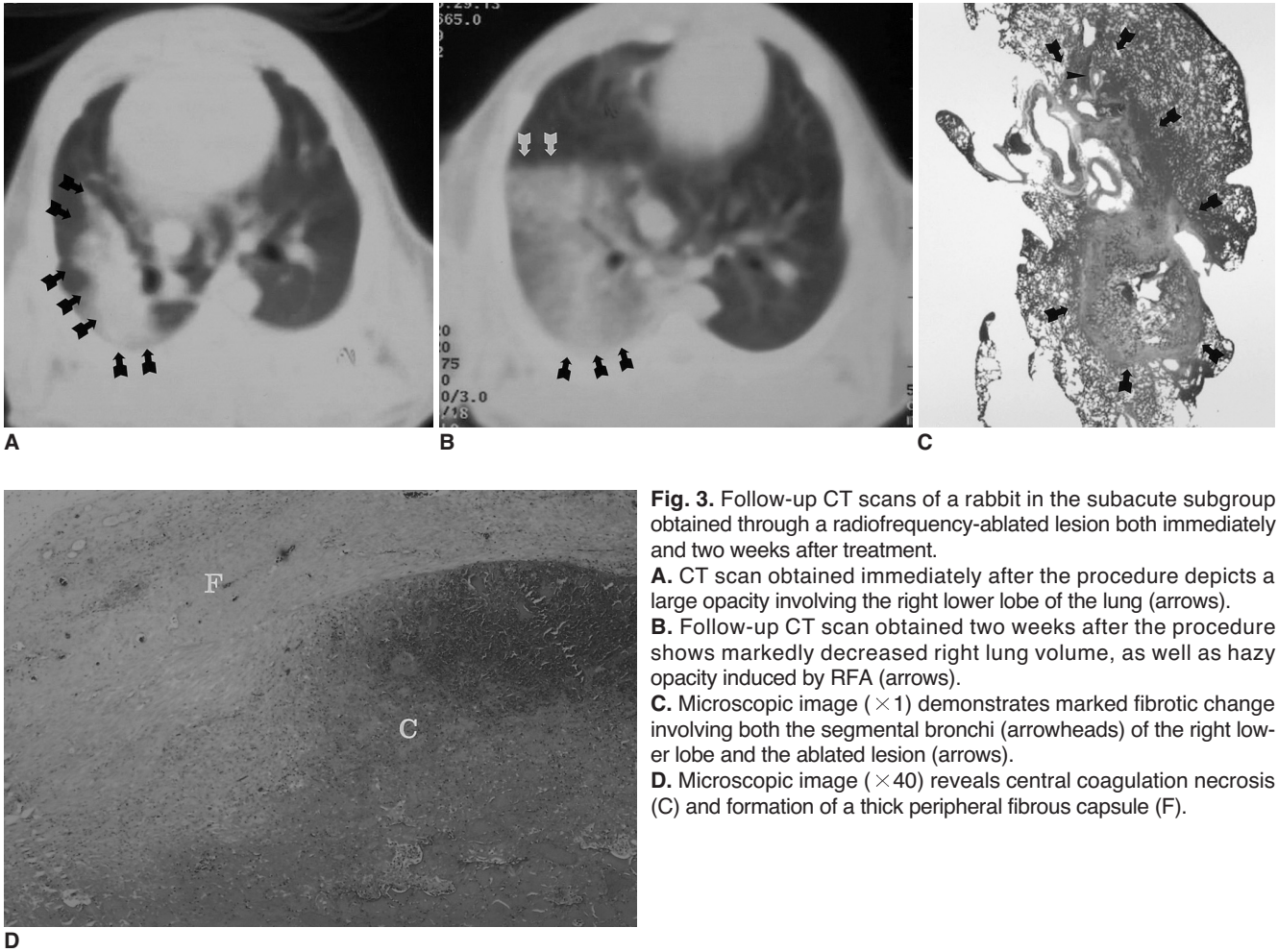


Fig. 3. Follow-up CT scans of a rabbit in the subacute subgroup obtained through a radiofrequency-ablated lesion both immediately and two weeks after treatment. **A.** CT scan obtained immediately after the procedure depicts a large opacity involving the right lower lobe of the lung (arrows). **B.** Follow-up CT scan obtained two weeks after the procedure shows markedly decreased right lung volume, as well as hazy opacity induced by RFA (arrows). **C.** Microscopic image ($\times 1$) demonstrates marked fibrotic change involving both the segmental bronchi (arrowheads) of the right lower lobe and the ablated lesion (arrows). **D.** Microscopic image ($\times 40$) reveals central coagulation necrosis (C) and formation of a thick peripheral fibrous capsule (F).

Table 2. Summary of Complications Related to Radio-Frequency Ablation Procedure

		Complication	p value
RFA group (n=10)			
Central lesions (n=5)		Large pneumothorax (n=2)	
Peripheral lesions (n=5)			
SRFA group (n=18)			p = .11*
Central lesions (n=9)		Large pneumothorax (n=1)	
		Small pneumothorax (n=1)	
		Hemothorax (n=1)	
Peripheral lesions (n=9)		Small pneumothorax (n=4)	p = .18 [†]
		Abscess (n=1)	
		Thermal injury to chest wall (n=2)	

Note.— *Difference between incidence rates of complications in the RFA and the SRFA group, [†]difference between incidence rates in complications in central and peripheral lesions in the SRFA group

vanced age (25). Those who are not candidates for surgery can undergo radiation treatment and/or chemotherapy, but survival prospects increase only modestly and gains are often accompanied by substantial toxicity, especially in patients suffering from other co-morbidities (26). Nevertheless, the development of nonsurgical and minimally invasive percutaneous techniques for the treatment of lung cancer would be advantageous. Effective options might prove useful for patients with multiple medical problems, co-morbid disease, or concomitant tumor, or for whom surgery carries high risks.

After encouraging results of RFA in the liver, some researchers have suggested that the procedure could be used for the treatment of lung malignancies (13–17). The main advantage of RFA is that it is simple, easy to perform and offers the option of an indefinite number of repeated applications. A drawback, however, is that it is often necessary to overlap ablations by multiple repositioning of the electrode in order to decrease marginal recurrence after RFA (6). Furthermore, if lung tumors are to be treated by RFA, the naturally high impedance of air-containing lung tissue and the risk of pneumothorax related to multiple passes through the pleura during RFA might be an obstacle to induction of complete tumor necrosis. If these inherent problems of RFA of lung tumors are to be solved, ablation must produce a larger coagulation area that could include focal lung malignancies and some safety margin. Several investigators have demonstrated the possibility of increasing RF tissue heating and coagulation during RF ablation by altering electrical and/or thermal conduction through the injection of saline into the tissues during RF application (18, 19). The present study was conducted to assess the actual effect of simultaneous infusion of saline during RFA, and possible resultant complications.

In our study, the mean diameter of RFA lesions in the saline infusion group was significantly greater than in the control group: 12.5 mm vs. 8.5 mm ($p < .05$). In addition, initial impedance in the SRFA group was significantly lower than in the RFA group ($p < .05$), and tissue impedance did not change markedly. Thus, in the SRFA group, high-RF energy instillation over a long period was possible, but in the RFA group, impedance changed rapidly during the procedure, frequently inducing activation of the pulsing technique. Furthermore, impedance was decreased by additional infusion of saline during the application of RF energy. This increases tissue ionicity and decreases tissue impedance, thereby permitting greater current flow, and the heated liquid spreads thermal energy further and faster through the tissue than does heat conduction (28, 29).

In this study, an internally cooled electrode was used for RFA, together with the pulsing technique, and the resultant

lesion was larger than that made by the conventional electrode used in previous studies (21, 27, 30). Nonetheless, even with an internal cooling mechanism and pulsing technique, impedance rose rapidly and uncontrollably during RF energy instillation, inducing frequent pulsing and leading to restrictions in the size of lesions. After saline infusion, however, the period of RF energy instillation increased, and with it, lesion size. Our results agreed with those of previous studies of saline-enhanced RFA of the liver and retroperitoneum (31–33). As demonstrated in this investigation, an extended volume of coagulation necrosis due to saline infusion may increase the clinical utility of RFA therapy by permitting successful treatment of larger lung tumors or reducing the number of sessions needed for the treatment of a given tumor. This finding is of particular importance in the application of RFA to the treatment of lung cancer, since in order to decrease the occurrence of pneumothoraces, electrodes should pass through the pleura as infrequently as possible. If the incidence of pneumothorax can be reduced, more patients may benefit from this potentially curative therapy, with its reduced medical and social costs.

Procedure-related complications arose in 12 cases, comprising eight pneumothoraces, two thermal injuries to the chest wall, one hemothorax, and one lung abscess (Table 2). Their incidence tended to be higher in the SRFA group (55.6%) than the RFA group (20%), though the difference was not statistically significant ($p = .11$). For the peripheral lesions, however, the complication rates among rabbits in the SRFA group (77.8%, 7/9) was higher than among those in the RFA group (0%) ($p < .05$). The relatively high incidence rates (28.6%, 8/28) of pneumothorax in this study were related to the small size of rabbit lung, the relatively large size of the electrodes, and the additional use of a Chiba needle with an electrode in the SRFA group. We believe that if the electrode used during RFA is adequate, permitting simultaneous instillation of saline during RFA in large animals or in clinical trials, the incidence rates of pneumothorax could decrease markedly.

Nevertheless, in a clinical setting, these potential problems require special attention. According to earlier reports of saline-enhanced RFA (18, 19, 31, 32), direct and uncontrollable thermal damage to both adjacent and remote structures was observed more frequently in the saline infusion group than in the conventional RFA group. To decrease this damage, we used a very small amount of saline (1.5 mL) at a slow infusion rate (approximately 0.05 mL/sec), and it is possible that the two cases of unexpected thermal injury to the chest wall and diaphragm resulted from drainage of steam or saline through low-resistance tissue. A further possible drawback of saline-enhanced RFA,

also involving this steam or saline drainage, is that the lesions produced may be somewhat irregular in shape, rather than spherical. However, most ablated lesions in the present study were spherical, and we believe that instillation of a larger amount of saline than we used could be related to the formation of irregularly shaped lesions.

The clinical role of RFA in the treatment of lung tumors is still not clear but will undoubtedly evolve. For example, in patients with hemoptysis or cough in whom radiotherapy has not controlled the symptoms or cannot be undertaken due to poor lung function or co-morbidity, this technique might play a primarily palliative role. We believe that in lung cancer patients, RF ablation possesses several potential benefits compared with systemic chemotherapy or radiotherapy. First, because the therapy is local in nature, it is likely to minimize damage to lung parenchyma and reduce adverse systemic effects on a patient's general health, and for this same reason, RF ablation therapy can be utilized in patients with limited pulmonary reserve. It is less likely to have a curative role for stage-I tumors because many patients with peripheral tumors who have poor lung function can be offered limited resection, such as wedge resection or segmentectomy by video-assisted thoracoscopic surgery (34–36). However, a randomized trial of lobectomy versus limited resection for stage-I lung cancer showed that the latter did not confer improved perioperative morbidity or mortality. Furthermore, even if less invasive than open surgery, limited resection also requires general anesthesia (35). There could, therefore, be a role for RFA as a less invasive alternative to metastasectomy, but for the present, the greatest clinical utility of RFA may be in patients with small peripheral lung cancers who are poor candidates for surgery.

Our study suffered certain limitations. First, the results obtained in healthy rabbit lung may differ from those obtained with non-small-cell human lung carcinoma. However, aspects of the process of cell degeneration caused by the effect of heat on tissue lead us to believe that the results might well be the same with either normal lung tissue in rabbits or human lung cancer cells. Second, rabbit lungs are smaller than the size of the RF ablation zone that can be produced with the currently available RF electrode system, and the effectiveness of saline infusion during RFA may thus not be entirely comparable between the two groups. In addition, since the 17-gauge electrode used in this study is too large for rabbits, with their relatively smaller lungs, the complication rates of RFA might be overestimated.

In conclusion, CT-guided percutaneous transthoracic RFA with simultaneous hypertonic saline infusion is feasible, and more effectively produces coagulation necrosis

than RFA without saline infusion. Saline-enhanced RFA might be a promising technique for the management of inoperable lung malignancies and has the potential for use as a minimally invasive approach. To determine whether the technique can be feasibly and safely used to produce a sufficiently large volume of necrosis to be of value in the treatment of small peripheral lung tumors in patients for whom surgery or palliative radiotherapy is unsuitable, further study using a larger animal model is warranted.

Acknowledgements

The authors wish to thank Seon OK Lee, R.T., for her assistance in animal observation and anesthesia, and her outstanding support in CT imaging. We also wish to acknowledge the editorial assistance of Bonnie Hami, M.A., Department of Radiology, University Hospital of Cleveland.

References

- Goldberg SN, Livraghi T, Solbiati L, Gazelle GS. *In-situ ablation of focal hepatic neoplasms*. In Gazelle GS, Saini S, Mueller PR, eds. *Hepatobiliary and pancreatic radiology: imaging and intervention*. New York: Thieme, 1997:470-502
- Curley SA, Izzo F, Ellis LM, Vauthey JN, Vallone P. Radiofrequency ablation of hepatocellular cancer in 110 patients with cirrhosis. *Ann Surg* 2000;232:381-91
- Curley SA, Izzo F, Delrio P, et al. Radiofrequency ablation of unresectable primary and metastatic hepatic malignancies: results in 123 patients. *Ann Surg* 1999;230:1-8
- Lim HK. Radiofrequency thermal ablation of hepatocellular carcinomas. *Korean J Radiol* 2000;1: 175-184
- Rossi S, Di Stasi M, Buscarini E, et al. Percutaneous RF interstitial thermal ablation in the treatment of hepatic cancer. *AJR Am J Roentgenol* 1996;167:759-768
- Dodd GD, Frank MS, Aribandi M, Chopra S, Chintapalli KN. Radiofrequency thermal ablation: computer analysis created by overlapping ablations. *AJR Am J Roentgenol* 2002;177:777-782
- Solbiati L, Ierace T, Goldberg SN, et al. Percutaneous US-guided radiofrequency tissue ablation of liver metastases: treatment and follow-up in 16 patients. *Radiology* 1997;202:195-203
- Sironi S, Livraghi T, Meloni F, Cobelli FD, Ferrero C, Maschio AD. Small hepatocellular carcinoma treated with percutaneous RF ablation: MR imaging follow-up. *AJR Am J Roentgenol* 1999;173:1225-1229
- Rosenthal DI, Hornicek FJ, Wolfe MW, et al. Percutaneous radiofrequency coagulation of osteoid osteoma compared with operative treatment. *J Bone Joint Surg Am* 1998;80:815-821
- Gervais DA, McGovern FJ, Wood BJ, et al. Radiofrequency ablation of renal cell carcinoma: early clinical experience. *Radiology* 2000;217:665-672
- Jeffrey SS, Birdwell RL, Ikeda DM, et al. Radiofrequency ablation of breast cancer: first report of an emerging technology. *Arch Surg* 1999;134:1064-1068
- Anzai Y, Lufkin R, DeSalles A, et al. Preliminary experience with MR-guided thermal ablation of brain tumors. *AJNR Am J Neuroradiol* 1995;16:39-48
- Zagoria RJ, Chen MY, Kavanagh PV, Torti FM. Radiofrequency ablation of lung metastases from renal cell carcinoma. *J Urol* 2001;166:1827-1828

Saline-Enhanced Radiofrequency Thermal Ablation of Lung

14. Dupuy DE, Zagoria RJ, Akerley W, Mayo-Smith WW, Kavanagh PV, Safran H. Percutaneous radiofrequency ablation of malignancies in the lung. *AJR Am J Roentgenol* 2000;174:57-59
15. Goldberg SN, Gazelle GS, Compton CC, McLoud TC. Radiofrequency tissue ablation in the rabbit lung: efficacy and complications. *Acad Radiol* 1995;2:776-784
16. Goldberg SN, Gazelle GS, Compton CC, Mueller PR, McLoud TC. Radiofrequency tissue ablation of VX2 tumor nodules in the rabbit lung. *Acad Radiol* 1996;3:929-935
17. Miao Y, Ni Y, Bosmans H, et al. Radiofrequency ablation for eradication of pulmonary tumor in rabbits. *J Surg Res* 2001;99:265-271
18. Livraghi T, Goldberg SN, Monti F, et al. Saline-enhanced radiofrequency tissue ablation in the treatment of liver metastases. *Radiology* 1997;202:205-210
19. Miao Y, Ni Y, Mulier S, et al. *Ex-vivo* experiment on radiofrequency liver ablation with saline infusion through a screw-tip cannulated electrode. *J Surg Res* 1997;71:19-24
20. Haaga JR. *Interventional CT-guided procedures*. In Haaga JR, Lanzieri CF, eds. *Computed tomography and magnetic resonance imaging of the whole body*. 3rd ed. St.Louis: Mosby, 1994:1572-1693
21. Goldberg SN, Stein M, Gazelle GS, Sheiman RG, Kruskal JB, Clouse ME. Percutaneous radiofrequency tissue ablation: optimization of pulsed-RF technique to increase coagulation necrosis. *J Vasc Interv Radiol* 1999;10:907-916
22. Lee JD, Lee JM, Kim SW, Kim CS, Mun WS. MR imaging-histopathologic correlation of radiofrequency thermal ablation lesion in a rabbit liver model: observation during acute and chronic stages. *Korean J Radiol* 2001;2:151-158
23. Ginsberg RJ, Vokes EE, Raben A. *Cancer of the lung: non-small cell lung cancer*. In Pass HI, Mitchell JB, Johnson DH, Turrisi AT, eds. *Cancer: principles and practice of oncology*. 5th ed. Philadelphia : Lippincott-Raven, 1996:849-857
24. Fry WA, Phillips JL, Menck HR. Ten-year survey of lung cancer treatment and survival in hospitals in the United States: a national cancer data base report. *Cancer* 1999;86:1867-1876
25. Downey RJ. Surgical management of lung cancer. *J Thorac Imaging* 1999;14:266-269
26. Moore DF, Jr, Lee JS. *Staging and prognostic factors: non-small cell lung cancer*. In Pass HD, Mitchell JB, Johnson DH, Turrisi AT, eds. *Lung cancer: principles and practice*. Philadelphia: Lippincott-Raven, 1996:481-494
27. Goldberg SN, Gazelle GS, Mueller PR. Thermal ablation therapy for focal malignancy: a unified approach to underlying principles, techniques, and diagnostic imaging guidance. *AJR Am J Roentgenol* 2000;174:323-331
28. Haines DE, Verow AF. Observations on electrode-tissue interface temperature and effect on electrical impedance during radiofrequency ablation of ventricular myocardium. *Circulation* 1990;82:1034-1038
29. Geddes LA, Baker LE. The specific resistance of biological material- a compendium of data for the biomedical engineer and physiologist. *Med Biol Eng* 1967;5:271-293
30. Gazelle GS, Goldberg SN, Solbiati L, et al. Tumor ablation with radio-frequency energy. *Radiology* 2000;217:633-646
31. Miao Y, Ni Y, Yu J, Marchal G. A comparative study on validation of a novel cooled-wet electrode for radiofrequency liver ablation. *Invest Radiol* 2000;35:438-444
32. Boehm T, Malich A, Goldberg SN, et al. Radio-frequency tumor ablation: internally cooled electrode versus saline-enhanced technique in an aggressive rabbit tumor model. *Radiology* 2002;222:805-813
33. Goldberg SN, Ahmed M, Gazelle GS, et al. Radio-frequency thermal ablation with NaCl solution injection: effect of electrical conductivity on tissue heating and coagulation – phantom and porcine liver study. *Radiology* 2001;219:157-165
34. Shennib HA, Landreneau R, Mulder DS, et al. Video-assisted thoracoscopic wedge resection of T1 lung cancer in high-risk patients. *Ann Surg* 1993;218:555-560
35. Landreneau RJ, Sugarbaker D, Mack MJ, et al. Wedge resection versus lobectomy for stage I (T1 N0 M0) non-small cell lung cancer. *J Thorac Cardiovasc Surg* 1997;113:691-700
36. Lung Cancer Study Group. Randomized trial of lobectomy versus limited resection for T1 N0 non-small cell lung cancer. *Ann Thorac Surg* 1995;60:615-623